Analysis of the Impact of Widespread Residential Heat Pumps and Photovoltaics on the Electricity Distribution Grid in Hamburg

Nicholas Tedjosantoso*, Martin Grasenack and Prof. Dr.-Ing. Hans Schäfers
Hochschule für Angewandte Wissenschaften Hamburg, Competence Center für Erneuerbare Energien und EnergieEffizienz (CC4E), Am Schleusengraben 24, 21029 Hamburg, Germany
*Nicholas.Tedjosantoso@haw-hamburg.de

Abstract

In this paper we discuss simulation results from a model developed to analyze the impact of household heat pumps (HP) and photovoltaics (PV) on the electricity distribution grid in Hamburg. Initially, the paper presents estimates of the future heat and electricity demand and PV-generated electricity, for residential buildings in Hamburg referring to existing studies and tools. Using a Linear Programming (LP) model, optimized electricity flows are calculated for the application of thermal and/or battery storage alongside the PV and HP installations in order to reduce the peak electricity loads for each individual building. To evaluate the results and the possible impacts on the electricity distribution grid, the results are aggregated based on their approximate location in relation to the medium-voltage (MV) supply areas. The results indicate that the effects of PV and HP on the electricity distribution grid are not evenly distributed and depend highly on the availability of a district heating solution.

Keywords – photovoltaic, heat pump, energy storage, district heating, sector coupling, linear programming

1 Introduction

By 2030, greenhouse gas emissions in Hamburg are to be reduced by 70 % compared to 1990. Hamburg is supposed to be completely climate-neutral by 2045 [1]. Such an undertaking requires the restructuring of the energy supply system as well as a vast expansion of the application of renewable energies. In an urban environment such as Hamburg, the largest photovoltaics (PV) potentials lie on rooftops of residential buildings [1]. Within residential buildings, a significant amount of energy is used for heating purposes. In the existing energy supply system, the largest part of the heating demand is covered using fossil energy [2]. To achieve the climate protection goals, a significant shift within the heat supply system towards a highly interconnected energy system is to be expected. Due to sector coupling, such a shift may result in problems within the electricity distribution grid.

2 Method

In this section, the methodology developed in this work is briefly explained. We begin with a brief overview of the workflow. Subsequently, the components of the workflow are explained in greater detail.

To study possible effects of widespread integration of PV and climate-friendly heating systems especially heat pumps (HP) in the residential building sector on the electricity distribution grid, a Linear Programming (LP) model was developed. This LP model considers only the physical and technical aspects of the system, while economical perspectives are ignored. Due to the detached nature of the residential heating system, outside of district heating solutions, the LP model is applied to each residential building individually. Considering the average wind generation, slightly higher PV yields and a slightly lower heat demand, 2011 has been chosen as a representative weather year to reflect the progression of climate change up to 2050 [3].

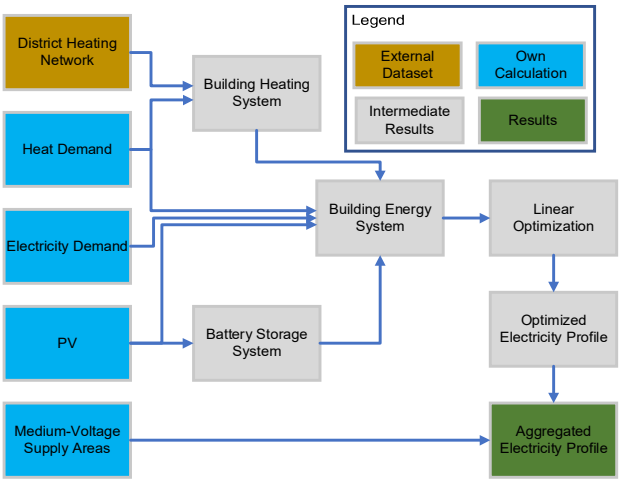

Figure 1 Simplified Workflow

Figure 1 depicts a simplified representation of the methodology developed in this study. The yellow rectangles signify input data sourced externally, while the blue rectangles denote input data generated within this study. The gray and green rectangles represent intermediate and final results produced within this research. The energy flow of a building is described by its electricity, heat, and PV generation time series. Depending on the location, the heat demand is met either by district heating or the building heating system. The size of the battery storage system is approximated using the capacity of the PV system. Using this information as input, the LP model then calculates the optimal electricity flow for the building energy system to minimize the peak electricity loads of each individual building. Finally, the results are aggregated for the medium-voltage (MV) supply areas which are supplied by a 110/10 kV transformer station.

2.1 Heat Demand

This section describes the method used to create hourly heat demand profiles for all the residential buildings. The methodology begins with the calculation of the reference area for residential buildings using building objects from ALKIS and the IWU (*Institut Wohnen und Umwelt*) building archetype [4], [5]. By employing TABULA's calculation method, the annual heat consumption can be determined [6]. This method was developed as part of the Hamburg Heat Demand Cadastre (*Wärmekataster*) and the GEWISS Project in Hamburg [7]. This methodology is preferably chosen over other established datasets, such as Peta5 [8], due to its spatial resolution (building-specific) and the regional scope of the project.

The calculated annual value for the heat demand is then disaggregated into daily values for the heat demand with the SigLinDe function [9] using weather data from the Hamburg Solar Potential Study [1]. Since SigLinDe deals with gas profiles, the assumption is made that the shape of the heat profile is identical to the gas profile, which has been widely used in grid planning and large-scale modeling of the German energy system [3]. Using intraday profiles generated as a part of the ego^n research project, the generated daily resolution can be further disaggregated into an hourly resolution of the heat demand. A total of roughly 460,000 profiles was derived and classified depending on the temperature class and building type [3]. Using this combination method, time series comprising of high spatial and high temporal resolution could be generated while maintaining a fully regional scope.

2.2 Electricity Demand

This section describes the methodology used to create electrical load profiles for all residential buildings in Hamburg, inspired by the ego^n project [3]. Instead of relying on standard load profiles (SLP), household-specific load profiles were derived. As part of the ego^n project, two sets of load profiles (2,511 and 100,000) categorized into 12 distinct household types, have been published. Employing these profiles instead of SLP we intended to overcome the inherent lack of variance and outdated measurements (from the 1980s) associated with SLPs.

To reduce computational time, this work utilizes the set of 2,511 profiles rather than the 100,000 generated profiles. To apply these load profiles, census dataset of 2011 is used. Due to different definitions of household types between the load profiles and the census, it is necessary to process and reorganize the census data set to ensure compatibility with the demand profiles. For this purpose, the methodology developed in ego^n is implemented to assign specific load profiles to each census cell depending on its household types [3].

Due to the mismatch between census and ALKIS in terms of publication date, namely 2011 and 2023, respectively, disaggregation of load profiles from census cells to ALKIS building would lead to residential buildings that have been inhabited or had been built after the year 2011 being excluded. As this primarily affects newer city districts, the effects are disproportionately distributed within the region.

In an effort to mitigate this problem, city district (*Stadtteile*) specific load profiles are generated. First, using ALKIS each census cell is assigned to a specific city district. Using the load profiles assigned to the cells, the annual electricity demand is calculated for the districts. For each city district, a scaling factor is introduced to ensure that the calculated annual electricity demand matches the annual demand, which is approximated using statistics of household structure in Hamburg [10] and the average electricity demand based on household size [11]. Using this methodology, a total of roughly 100 city district-specific load profiles is generated. The scaled profiles are finally allocated to each residential building based on its assumed reference area (living space).

2.3 PV Generation

The estimation of PV generation profiles begins with the estimation of the available roof area for all residential buildings in Hamburg using ALKIS and the 3D LoD2 dataset for the city, both of which are periodically updated and published under an open data license [12]. These datasets allow for the classification of each roof area based on its characteristics, including tilt angle, orientation, and surface area. These characteristics are subsequently used to assess the feasibility of PV installation based on a set of criteria.

The first criterion involves the gross roof area available on any respective building. Buildings with less than 50 m² of gross roof area are assumed to lack PV capacity. Due to the possibility of a building to have multiple roof sections, another criterion is introduced to examine the suitability of every section of the roof surface. For buildings with more than 50 m² gross roof area, flat roof sections smaller than 20 m² and tilted roof sections smaller than 10 m² are deemed unsuitable for PV. These simplified assumptions are based on the obligation to install PV systems in Hamburg since 2023 [13].

To ensure the economic and energetic viability of the assumed PV installation, a constraint regarding the minimum irradiation level is implemented. Long-term averages (2001-2020) generated in the solar potential study conducted in Hamburg are utilized for this purpose [1]. In this work, the minimal annual yield is set to 80 % of the optimal configuration, providing a buffer compared to the legal requirement [13]. Figure 2 illustrates the long-term average annual PV solar yield depending on tilt angle and azimuth.

To model the PV potential, a methodology developed in the solar potential study is implemented, which resulted in the following assumptions. A surface utilization factor of 80 % is applied to flat roofs, while 60 % is set for tilted roofs. Furthermore, PV modules on flat roofs are modeled with a 15° inclination and an east/west orientation [1]. The amount of PV installed on each roof surface is determined using a power density of 200 W/m² [1]. To model the

losses, a performance ratio of 80 % is uniformly implemented for each time step [1]

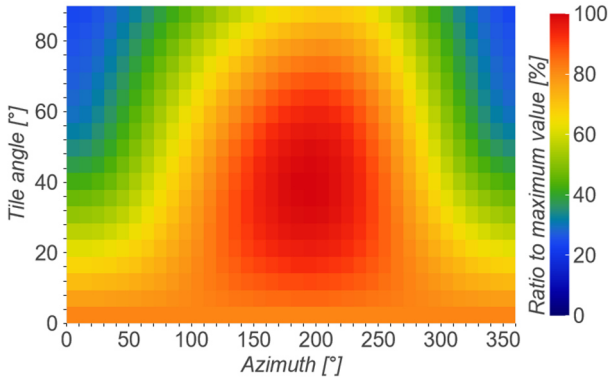

Figure 2 Long-term average annual PV yield. 0° azimuth represents north [1]

2.4 Building Energy System

Within this work, a number of assumptions are utilized to model the individual building energy systems, which can be categorized into two sectors: electricity and heat. Regarding electricity, it is assumed that the building is connected to the electricity grid. Depending on the availability of district heating networks for the respective building objects, different assumptions are made concerning the heating system. If district heating is available, it is assumed that the building's heat demand can be entirely met by district heating at all times. Otherwise, the heat demand is met using its own heating system. Figure 3 illustrates a simplified representation of the building energy system utilized in this work.

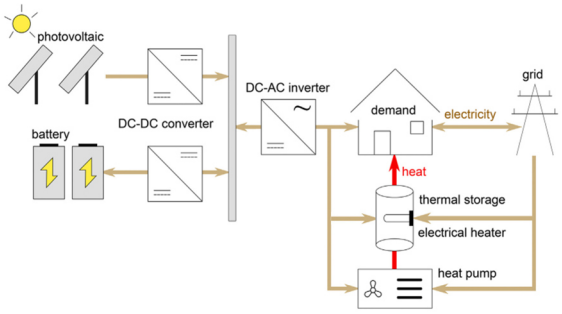

Figure 3 Building energy system. Taken from [14]

2.4.1 Battery Storage System

In this work, a fixed ratio of 1.5 kWp/kWh between the installed PV power in kW and the battery capacity in kWh is utilized to estimate the battery capacity [15]. Despite recent improvements in battery storage systems, it is important not to overlook the losses inherent in such systems. Depending on the possible energy conversion paths, different efficiency values are used [16]. Furthermore, a daily self-discharge rate of 0.17 % is assumed [17]. Table 1 provides an overview of the assumed battery losses. Within this work, a maximum C-Rate of 1C for both charge and discharge is assumed. Additionally, the battery storage system is allowed to be charged from both the grid and PV.

Table 1 Battery efficiency and losses [16, 17]

Loss Type	Value	Source
PV to Battery	95.8 %	[16]
PV to Grid	96.2 %	[16]
Battery to Grid	95.5 %	[16]
Grid to Battery	95.3 %	[16]
Daily self discharge	0.17 %	[17]

2.4.2 Heating System

As the combination of a HP, electrical heater, and thermal energy storage (TES) is employed to meet the assumed heat demand of the building, sizing these components is crucial for ensuring a cost-effective operation. In literature, sizing is often achieved through technical guidelines and standards (e.g., VDI 4645 and DIN/TS 12831) or mathematical optimization. However, these options are not suitable for the large number of building objects considered in this work due to the extensive efforts required for such calculations. As a simplification, the SIZEP (Sizing Evaluation Step) method described in [18], originally developed for use in combination with combined heat and power (CHP) plants, is used to estimate the capacity and power of TES.

SIZEP relies solely on time-series data (historical heat load) to approximate the capacity of thermal energy storage independently of the heat source. For this approximation, two descriptive parameters are derived out of the time-series, namely: RHV (relative hourly variation) and DAHV (daily accumulated heat volume). These calculations require the calculation of annual average heat load (L_a), daily average heat load (L_d), hourly average heat load (L_h). The equations are shown below.

$$RHV = \frac{|L_h - L_d|}{L_a} \cdot 100 \quad (1)$$

$$DAHV = \frac{\sum_{h=1}^{24} |L_h - L_d|}{2} \quad (2)$$

Using the first parameter RHV, the variation of the heat load in each hour of the year can be characterized to provide an approximation of the power required for thermal energy storage to eliminate the hourly load variation during a day [18]. This value is then multiplied by the annual average heat load to determine the heating load of the heat pump. The calculation assumes that the thermal power of the thermal energy storage is equal to the heating load of the heat pump. The second parameter, DAHV, provides an approximation of the necessary thermal storage capacity to ensure the continuous operation of the CHP plant over 24 consecutive hours throughout the entire year [18]. To consider outliers, the 99th percentile is used for RHV and DAHV instead of their maximum values.

Within this work, heat pumps are modeled using a coefficient of performance (COP) that varies with temperature, as the COP of a heat pump depends highly on the temperature of its heat source. To model this temperature dependency, the formula provided in [19] for air-source heat pumps is utilized. Since this work exclusively focuses on

air-source heat pumps, ambient temperature data from the solar potential study conducted in Hamburg is used as the heat source temperature (T_{so}). The sink temperature (T_{si}) in this study is assumed to be 50°C [20].

$$\Delta T = T_{si} - T_{so} \quad (3)$$

$$COP = 6.81 - 0.121 \cdot \Delta T + 0.00063 \cdot \Delta T^2 \quad (4)$$

In the context of this work, electrical heaters serve as an additional heat source and are assumed to operate with 100 % efficiency. Given that the primary purpose of these electrical heaters is to provide heating support, their size is left as a decision variable in the optimization model.

Similar to battery storage systems, the consideration of losses within the TES is simplified using a set of constant values. A 90 % efficiency for both charge and discharge, along with a daily self-discharge rate of 0.5 %, is implemented [17]. Furthermore, TES can be charged using both electrical heater and heat pump.

2.5 District Heating Areas

As previously mentioned, the assumed heating system of a building depends on the availability of district heating. In this study, the district heating dataset was generated as part of a study to examine whether and how climate-neutral housing can be achieved in Hamburg by 2045 [21]. Figure 4 provides an overview of the district heating dataset used in this work.

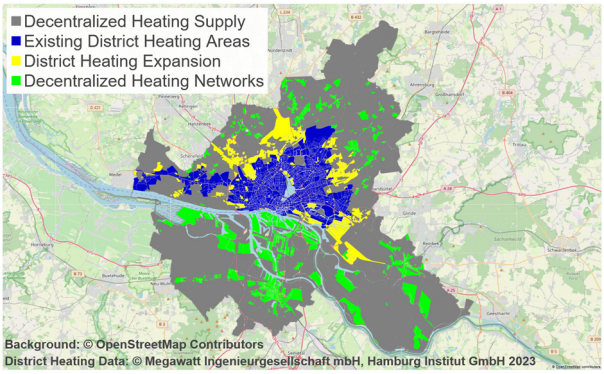

Figure 4 District heating areas [21], [22]

Since this study aims to analyze the heating structure of residential buildings in Hamburg in their final carbon-neutral state, carbon-neutral district heating is assumed to also be available for both district heating expansion and decentralized heating network areas. By combining the district heating dataset with the approximate building locations based on ALKIS, the heating system of each building can be determined.

2.6 Medium-Voltage Supply Area

To analyze the impact of residential heat pumps and PV on the electrical distribution grid in Hamburg, georeferenced grid datasets are required. Efforts have been made in the literature to generate synthetic MV supply areas in Germany using open data [23]. However, due to the nationwide scope of such projects, the accuracy of the results may be insufficient to accurately model a specific region such as Hamburg. In this work, the MV supply area for Hamburg is approximated based on scalable vector graphics (SVG) available on the website of Stromnetz Hamburg. As this graphic is no longer publicly accessible, an archived version from June 2022 is utilized [24].

Due to the characteristics of SVG graphics, a georeferencing process is required before this graphic can be used. Georeferencing is achieved using administrative borders from ALKIS as control points. Due to the quality of the SVG graphic and the manual selection of the control points, inaccuracies within individual areas of the MV supply area are to be expected. These supply areas represent the supply areas of 110/10 kV transformer stations in Hamburg. The resulting georeferenced MV supply area is shown in Figure 5.

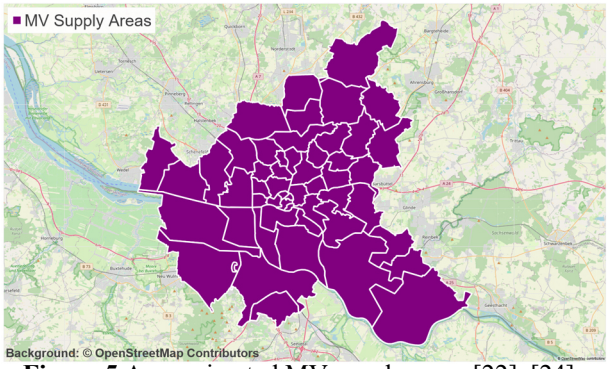

Figure 5 Approximated MV supply areas [22], [24]

Within this work, the supply area of Altenwerder and Hausbruch are assumed to have no residential buildings, as both zones are comprised almost exclusively of port and industrial areas.

2.7 Optimization Model

Following the aim of this work, the LP model implemented in this work is designed to optimize the energy flow of the building from the point of view of the distribution system operator (DSO). This results in the optimization of the peak electricity taken from and fed into the grid, while ensuring the heat demand of the building is met at all times. In the following, the assumptions and equations used for this model are explained briefly.

The overall heat balance (W_{th}) of the building is defined by equation 5. The heat demand is met using the combination of an electrical heater (W_{elh}), a heat pump (W_{hp}) and energy discharged from TES ($W_{TES,d}$), while considering the discharge efficiency of the TES (η_{TES}).

$$\mathrm{W_{th}}[t] = \mathrm{W_{hp}}[t] + \mathrm{W_{elh}}[t] + W_{TES,d} \cdot \eta_{TES} \quad (5)$$

The energy stored at the start of the time step (W_{TES}) is calculated using equation 6, with $W_{TES,c}$ representing the amount of energy charged and $W_{TES,d}$ the amount of energy discharged from the storage system. As this work assumes a constant daily self-discharge rate (σ_{TES}) regardless of the boundary condition, this value is divided by 24 to calculate the hourly self-discharge rate. Furthermore, it is assumed that initially ($t = 0$), no amount of thermal energy is stored in the storage system.

$$\mathrm{W_{\Delta TES}}[t] = \begin{matrix} W_{TES}[t-1] + \\ W_{TES,c}[t-1] - \\ W_{TES,d}[t-1] \end{matrix} \quad (6)$$

$$W_{TES}[\mathrm{t}] = \quad (W_{\Delta TES}[t]) \cdot \left(1 - \frac{\sigma_{TES}}{24}\right) \tag{7}$$

To simplify the charge and discharge process, the assumption is made that the amount of energy available for charging and discharging is limited by the heat amount stored at the beginning of the time step. Furthermore, the simplification that thermal storage can be charged and discharged simultaneously is used.

$$W_{TES,c}[\mathrm{t}] \leq \left(W_{TES,max} - W_{TES}[t]\right) \tag{8}$$

$$W_{TES,d}[\mathrm{t}] \leq W_{TES}[t] \tag{9}$$

The amount of heat added to thermal energy storage depends on the heat added from the heat pump ($W_{hp,c}$) and the electrical heater ($W_{elh,c}$), taking into account losses (η_{TES}). The corresponding electrical energy required for this process depends on the electricity sourced from the battery storage ($W_{BAT,d,TES}$), PV ($W_{PV,TES}$), or the electricity grid ($W_{grid,TES}$). The electricity demand of the heat pump corresponds to its COP.

$$W_{TES,c}[t] = \left(W_{\mathrm{hp,c}}[t] + W_{elh,c}[t]\right) \cdot \eta_{TES} \tag{10}$$

$$\frac{W_{hp,c}[\mathrm{t}]}{COP[t]} + W_{elh,c}[t] = \begin{matrix} W_{BAT,d,TES}[t] \cdot \eta_{\mathrm{BAT2AC}} + \\ W_{PV,TES}[\mathrm{t}] \cdot \eta_{\mathrm{PV2AC}} + \\ W_{\mathrm{grid,TES}}[t] \end{matrix} \tag{11}$$

To ensure that the total heat produced by the heat pump does not exceed its maximum capacity, the following equation is introduced.

$$W_{hp}[\mathrm{t}] + W_{hp,c}[t] \leq \mathrm{W}_{hp,max} \tag{12}$$

Similar to the assumptions used for TES, the battery is assumed to be empty at the start. The amount of electrical energy available in the battery (W_{BAT}) at a particular time step depends on the stored energy and the energy flow of the battery ($W_{BAT,c}$ and $W_{BAT,d}$) from the previous time step. The battery storage also considers a constant self-discharge rate (σ_{BAT}). Simplifications regarding charging and discharging are also implemented, as for the TES.

$$W_{\Delta BAT}[\mathrm{t}] = \begin{matrix} W_{BAT}[t-1] + \\ W_{BAT,c}[t-1] - \\ W_{BAT,d}[t-1] \end{matrix} \tag{13}$$

$$W_{BAT}[\mathrm{t}] = \quad (W_{\Delta BAT}[t]) \cdot \left(1 - \frac{\sigma_{BAT}}{24}\right) \tag{14}$$

$$W_{BAT,c}[\mathrm{t}] \leq \left(W_{BAT,max} - W_{BAT}[t]\right) \tag{15}$$

$$W_{BAT,d}[\mathrm{t}] \leq W_{BAT}[t] \tag{16}$$

Since no limitations are placed on the source of electricity to charge the battery, both PV ($W_{PV,BAT}$), and electricity from the grid ($W_{grid,BAT}$), can be utilized. Assumptions from Table 1 are used for each of the energy paths.

$$W_{BAT,c}[t] = \begin{matrix} W_{PV,\mathrm{BAT}}[t] \cdot \eta_{PV2BAT} + \\ W_{grid,BAT}[t] \cdot \eta_{AC2BAT} \end{matrix} \tag{17}$$

Depending on its usage, the amount of electricity discharged from the battery is split into two parts.

$$W_{BAT,d}[\mathrm{t}] = W_{BAT,d,grid}[t] + W_{BAT,d,TES}[t] \tag{18}$$

Within this work, no distinction is made between electricity used for demands in the building and for grid feed-in, as from the point of view of the DSO, both possibilities reduce the electricity taken from the grid. These assumptions result in the following equation for PV generation.

$$W_{PV}[\mathrm{t}] = \begin{matrix} W_{PV,BAT}[t] + \\ W_{PV,TES}[t] + \\ W_{PV,grid}[t] \end{matrix} \tag{19}$$

In regards to the total electricity demand ($W_{el,t}$), the difference between the electricity required from and fed into the grid is calculated. This results in the following equation.

$$W_{el,t}[\mathrm{t}] = \begin{matrix} W_{el,buildng}[t] + \\ \frac{W_{hp}[t]}{COP[t]} + W_{elh}[t] + \\ W_{grid,BAT}[t] + W_{grid,TES}[t] - \\ W_{BAT,d,grid}[t] \cdot \eta_{BAT2AC} - \\ W_{PV,grid}[t] \cdot \eta_{PV2AC} \end{matrix} \tag{20}$$

However, the chosen optimization model can lead to an unrealistically high total electricity demand. This occurs because the optimization model used does not consider the economic aspect of the energy system, treating electricity from the grid as free of charge. To mitigate this problem, an annual limit ($W_{el,lim}$) is set for $W_{el,t}$. $W_{el,lim}$ represents the total electricity demand for the building, assuming that the heat demand is met using only the heat pump and electrical heater without storage options and PV installation. This results in the following equation.

$$\sum_{\forall t \in T} W_{el,t} \leq W_{el,lim} \tag{21}$$

To prevent this LP model from becoming a multi-objective optimization model, the total electricity demand is split into its positive ($W_{el,+}$) and negative ($W_{el,-}$) components due to the presence of PV. The objective function (Z) can then be formulated using (22) to minimize the sum of the highest positive component and the highest absolute value of the negative component.

$$Z = \mathrm{minimize}\left(\max\left(W_{el,+}\right) + \max\left(\left|W_{el,-}\right|\right)\right) \tag{22}$$

3 Plausibility Test

To assess the extent of errors made using the presented methods, plausibility tests are conducted. However, due to the lack of available data, these tests can only be performed for a limited number of generated datasets and using publicly available datasets for comparison.

3.1 Reference Area

As both the estimation of electricity and heat demand depends on the estimation of the buildings estimated living area, the reference area provides a first estimation, whether the methods presented is plausible. The test is based on methods described in [7], using data from the Hamburg statistics office, which contains average residential living space per city district [10]. By employing a linear regression fitting, a good fit is achieved ($y = 0.987x$ and $r^2 = 0.974$). Overall, the estimated residential living area shows an overestimation of 0.2 % compared to the statistically available living area. Despite the good correlation between the aggregated values, significant deviations will occur at

the individual building level, due to the aggregated nature of the available datasets.

3.2 Annual Heat Demand

A plausibility test for the annual heat demand is done using a similar aggregated approach with a focus on the overall heating demand for the whole region of Hamburg. Using methods described in [8], reference values for comparison have been calculated using the available statistics from Hamburg statistics office and AGEB, deriving the total heat demand for Hamburg [10], [25]. To ensure that the calculated values from statistics are comparable with the methodology used in this work, weather correction using degree days is used [7]. The annual heat demand from the heat demand model is finally compared to the calculated average annual demand for years 2019-2021 from the statistics [7], [10], [25]. From the results in Table 3, the model used in this work is plausible. It is nonetheless important to note that the values calculated from the energy statistics provide only an aggregated approximation and should therefore be approached with care.

Table 3 Comparison of estimated annual heat demand and energy statistics.

Source	Total Heat Demand [GWh/a]
Three Year Average of HH	10,253
Heat Demand Model	10,274

3.3 Annual Electricity Demand

As no publicly available data set for the annual electricity demand of the residential sector is available, this value needs to be estimated using available statistics. For this reason, the methodology used to estimate the annual heat demand is transferred to the electricity sector [7], [10], [25]. The result of this comparison is shown in Table 4. The model used in this work overestimates the electricity demand by roughly 5.6 % and is deemed acceptable for the scope of this work.

Table 4 Comparison of estimated annual electricity demand and energy statistics.

Source	Total Electricity Demand [GWh/a]
Three Year Average of HH	2,611
Electricity Demand Model	2,757

3.4 Hourly Heat Load Profile

The assessment of the hourly heat demand time series presented in this work is conducted by comparing its hourly values to the Standard Load Profile (SLP) for gas at the NUTS-1 level, which has often been used as a proxy for heat demand profiles [3], [26]. To ensure comparability with the calculated load profile, the SLP is scaled to the same annual demand as the calculated profile. Table 5 shows that both profiles are relatively similar, with the main differences observed in their peak values.

Table 5 Statistical overview of the SLP gas [26] and heat demand model.

	SLP [MWh/h]	Model [MWh/h]
Median	971	983
Min	21	12
Max	4,401	3,358
Standard Deviation	835	842

3.5 Hourly Electricity Load Profile

To assess the plausibility of the generated hourly electricity time series, a comparison is made with the Standard Load Profile (SLP) [27]. Due to the lack of measurement data, this comparison is made at the NUTS-1 level. Table 6 provides a statistical overview of both profiles. From this table, it is observed that the electricity demand model generates higher peak values with higher standard deviations.

Table 6 Statistical overview of the SLP [27] and electricity demand model.

	SLP [MWh/h]	Model [MWh/h]
Median	329	297
Min	102	55
Max	732	956
Standard Deviation	134	211

Comparison of both profiles furthermore shows, that while the peaks in demand align in time, a considerable difference in magnitude can be observed. Considering that the Standard Load Profiles (SLP) are based on measurements made in the 1980s and 1990s, the difference in peak values also aligns with the technological development (e.g., lower stand-by consumption) of household appliances since the development of the profiles [3], [27]. Taking these factors into account, this deviation is deemed acceptable.

4 Results

To study the potential effects of the implemented technologies on the electricity distribution grid, the optimization results are aggregated at the MV level based on their location. To interpret the results, full load hours (FLH) are calculated by dividing the sum of the annual absolute electricity demand by the peak absolute electricity demand. Low FLH correspond to a relatively volatile electricity demand profile with high peak values, while high FLH refer to a relatively even electricity profile. Figure 8 shows the result of this assessment, indicating that high FLH values are mostly located outside of the city center. Within this work, the difference between residential buildings located within and outside of the city center mainly is related to their heating system.

Buildings closer to the city center are connected to the district heating grid more often. In this study they are equipped with PV and battery storage. Buildings outside are equipped with heat pumps (in most cases), thermal storage, battery storage, and PV.

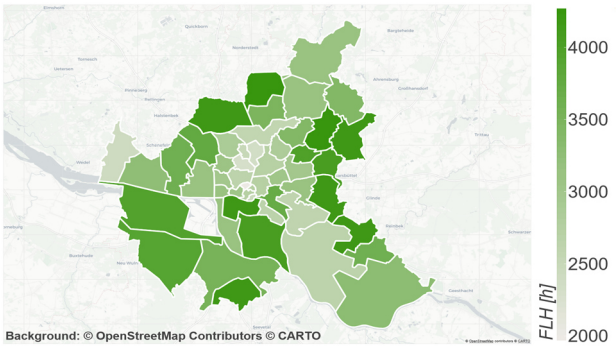

Figure 8 FLH on MV supply area [22]

By overlapping the MV supply areas and district heating areas in Figure 9, a correlation between supply areas and low FLH can be found. Figure 9 illustrates that low FLH values are mainly located in areas where a high degree of district heating connection is expected, which within this work is translated to the absence of a heat pump, electrical heater, and thermal energy storage in these areas.

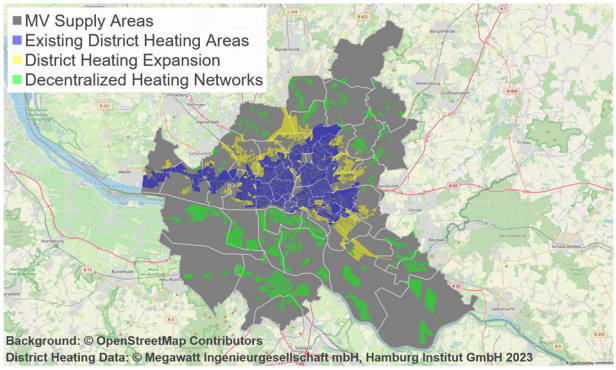

Figure 9 Overlap MV supply areas and district heating areas [21,22]

To further illustrate effects caused by the different heating system, a four-story multi-family residential building located in the city district Schnelsen is used as an example. Using the method described in Section 2.3 and 2.4.1, sufficient roof surface is available for PV usage with battery storage system. For illustration purposes, the optimization model for this building is implemented twice using different heating system assumptions, namely district heating network in the first (green) and a building heating system with a heat pump and thermal storage in the second (red) case. The result of this optimization is shown in Figure 10.

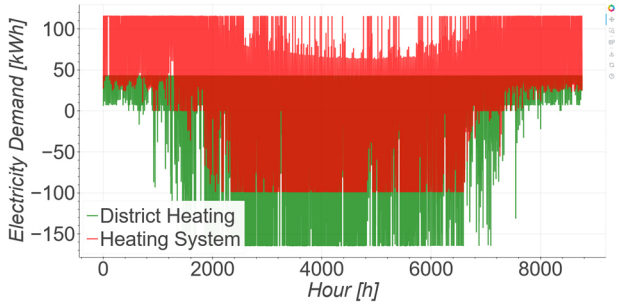

Figure 10 Hourly electricity demand depending on the heating system

When the heat is supplied by district heating (green), it can be seen that, even with the optimized use of battery storage, the peak generation in summer (negative demand values representing generation) is significantly higher (up to appr. 150 kW) than the peak demand in winter (appr. 40 kW). For the combination of HP, TES, and electrical heater (red), it can be clearly seen that the peak demand in winter (appr.115 kW) and the peak generation in summer (appr. 100 kW) are closer in their absolute value.

To evaluate the proportion of the residual feed-in provided by PV generation, the ratio between the peak demand and peak generation is calculated. With a ratio of 1.17 for an HP based heating system compared to 0.26 for a district heating based system, the potential of sector coupling to mitigate the seasonal volatility of PV generation is further emphasized.

5 Conclusion

From Figures 8, 9, and 10, it is evident that maintaining the stability of the electricity grid requires a significant degree of flexibility and storage to mitigate short-term fluctuations in both energy consumption and generation. Furthermore, it can be seen, that the detrimental effects of PV generation cannot be evenly prevented. The widespread deployment of rooftop PV systems might present challenges, characterized by highly volatile and a seasonal bidirectional electricity flows especially in areas with little sector coupling and/or without thermal and battery storage means.

Moreover, the combination of district heating and high PV penetration in residential areas poses potential challenges, as the beneficial coupling between the electricity and heat sectors may be reduced, leading to increased seasonal volatility of PV generation in these areas. Compared to the city center, the flexibility offered by HP, TES, and electrical heater on the outskirts of the city provides an opportunity to integrate PV generation without placing a disproportionate burden on the electricity grid during the summer.

Given the scope of this work, the model used here is simplified, focusing primarily on technical aspects. However, future research should consider integrating economic considerations and conducting a comprehensive analysis of other sectors to provide a more accurate assessment of the impacts of these technologies on the electricity grid.

6 References

[1] C. Rullán Lemke, D. John, N. Tedjosantoso, M. Kaltschmitt, H. Schäfers, and C. Lange, “Solarpotenzialsstudie für Hamburg”, Erneuerbare Energien Hamburg Clusteragentur GmbH, Hamburg, 2023.

[2] Destatis. “Energy consumption for housing, by energy source”. destatis.de. Accessed: 02.01.2024, [Online]. Available: https://www.destatis.de/EN/Themes/Society-Environment/Environment/Environmental-Economic-Accounting/_Graphic/_Interactive/energy-consumption-housing-energy.html

[3] C. Buttner et al., “Open modeling of electricity and heat demand curves for all residential buildings in germany”, Energy Informatics, vol. 5, no. S1, 2022-09. DOI: 10.1186/s42162- 022- 00201- y.

[4] LGV, “Alkis - ausgewählte Daten Hamburg” Hamburg, Germany, 2023. [Online]. Available: https://metaver.de/trefferanzeige?docuuid=DC71F8A1-7A8C-488C-AC99-23776FA7775E#detail_links

[5] T. Loga, B. Stein, N. Diefenbach, and R. Born, “Deutsche Wohngebaudetypologie: Beispielhafte Maßnahmen zur Verbesserung der Energieeffizienz von typischen Wohngebauden,” 2015. [Online]. Available: https://www.episcope.eu/downloads/public/docs/brochure/DE_TABULA_TypologyBrochure_IWU.pdf

[6] IWU, “Tabula calculation method – energy use for heating and domestic hot water,” 2013. [Online]. Available: https://www.episcope.eu/downloads/public/docs/report/TABULA_CommonCalculationMethod.pdf

[7] I. Dochev, H. Seller, and I. Peters, “Assigning energetic archetypes to a digital cadastre and estimating building heat demand. an example from hamburg, germany”, Environmental and Climate Technologies, vol. 24, no. 1, pp. 233–253, 2020-01. DOI:10.2478/rtuect-2020-0014

[8] B. Möller, E. Wiechers, L. Sánchez-García, and U. Persson, “D5.7: Spatial models and spatial analytics results,” 2022. [Online]. Available: https://zenodo.org/records/6524594

[9] M. Hinterstocker, B. Eberl, and S. von Roon, “Weiterentwicklung des Standardlastprofilverfahrens Gas”, 2015. [Online]. Available: https://www.ffe.de/wp-content/uploads/2022/08/Studie_Weiterentwicklung-SLP-Gas_FfE.pdf

[10] Statistik Nord, “Statistisches Amt für Hamburg und Schleswig-Holstein,” statistic-nord.de. Accessed: 18.11.2023 [Online]. Available: https://www.statistik-nord.de/

[11] bdew, “Energieeffizienz”, bdew.de. Accessed: 14.11.2023, [Online]. Available: https://www.bdew.de/presse/pressemappen/faq-energieeffizienz/

[12] LGV, “Metadaten Verbund (MetaVer),” metaver.de. Accessed: 26.11.2023 [Online]. Available: https://metaver.de/startseite

[13] BUKEA. “Klimafreundliche EnergiePhotovoltaik ist Pflicht in Hamburg,” hamburg.de. Accessed: 14.11.2023 [Online]. Available: https://www.hamburg.de/energielotsen/beratung/15147914/faqs-photovoltaikanlagen-pflicht/

[14] D. Coppitters, W. De Paepe, and F. Contino, “Robust design optimization of a photovoltaic battery-heat pump system with thermal storage under aleatory and epistemic uncertainty”, Energy, vol. 229, p. 120 692, 2021-08. DOI: 10.1016/j.energy.2021.120692

[15] B. Boeckl and T. Kienberger, “Sizing of PV storage systems for different household types”, Journal of Energy Storage, vol. 24, p. 100 763, 2019-08. DOI: 10.1016/j.est.2019.100763

[16] N. Orth, J. Weniger, L. Meissner, I. Lawaczeck, and V. Quaschning, “Stromspeicher-inspektion 2022“, HTW Berlin, Berlin, Germany, 2022. [Online]. Available: https://solar.htw-berlin.de/wp-content/uploads/HTW-Stromspeicher-Inspektion-2022.pdf

[17] A. A. Kebede, T. Kalogiannis, J. Van Mierlo, and M. Berecibar, “A comprehensive review of stationary energy storage devices for large scale renewable energy sources grid integration”, *Renewable and Sustainable Energy Reviews*, vol. 159, p. 112 213, 2022-05. DOI: 10.1016/j.rser.2022.112213

[18] P. Benalcazar, “Sizing and optimizing the operation of thermal energy storage units in combined heat and power plants: An integrated modeling approach”, Energy Conversion and Management, vol. 242, p. 114 255, 2021-08. DOI: 10.1016/j.enconman.2021.114255

[19] T. Brown et. al., “Synergies of sector coupling and transmission reinforcement in a cost-optimised, highly renewable european energy system”, Energy, vol. 160, pp. 720–739, 2018-10. DOI: 10.1016/j.energy.2018.06.222

[20] M. Lammle, C. Bongs, J. Wapler, ¨ et al., “Performance of air and ground source heat pumps retrofitted to radiator heating systems and measures to reduce space heating temperatures in existing buildings”, Energy, vol. 242, p. 122 952, 2022-03. DOI: 10.1016/j.energy.2021.122952

[21] Megawatt Ingenieurgesellschaft mbH and Hamburg Institut GmbH, *Gutachten Energetische Quartiersentwicklung*, de, Behorde für Stadtentwicklung und Wohnen (BSW), 2023.

[22] OpenStreetMap contributors, 2024, “OpenStreetMap“ [Online]. Available: https://www.openstreetmap.org.

[23] J. Amme, G. Pleßmann, J. Buhler, L. Hülk, E. Kötter, and P. Schwaegerl, “The ego grid model: An open-source and open-data based synthetic medium-voltage grid model for distribution power supply systems”, *Journal of Physics: Conference Series*, vol. 977, p. 012 007, 2018-02. DOI: 10.1088/1742-6596/977/1/012007

[24] Stromnetz Hamburg. “Übersicht der Umspannwerksreserven,” energieportal-hamburg.de. Acessed: 22.06.2022. [Online]. Available: https://www.energieportal-hamburg.de/uw-reserven

[25] AGEB, “Anwendungsbilanzen zur Energiebilanz Deutschland: Endenergieverbrauch nach Energietragern und Anwendungszwecken”, 2023. [Online]. Available: https://ag-energiebilanzen.de/wp-content/uploads/2023/01/AGEB_21p2_V3_20221222.pdf

[26] BDEW/VKU/GEODE, Leitfaden “Abwicklung von Standardlastprofilen Gas”, 2022. [Online]. Available: https://www.bdew.de/media/documents/20220331_LF_SLP_Gas_KoV_XIII_3Qo7qMf.pdf

[27] H. Meier, C. Funfgeld, T. Adam, and B. Schieferdecker, “Repräsentative VDEW-Lastprofile”, VDEW, Frankfurt (Main), 1999. [Online]. Available: https://www.bdew.de/media/documents/1999_Repraesentative-VDEW-Lastprofile.pdf